

Hydrophobic and Metal-Coordinated Confinement Effects Trigger Recognition and Selectivity

Hui-Bin Zhang, Kuppusamy Kanagaraj, Julius Rebek, Jr., and Yang Yu*



Cite This: *J. Org. Chem.* 2021, 86, 8873–8881



Read Online

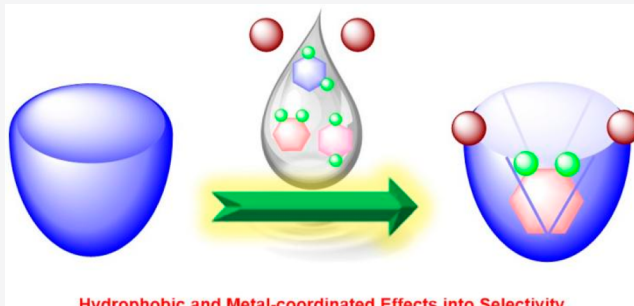
ACCESS |

Metrics & More

Article Recommendations

Supporting Information

ABSTRACT: We report the synthesis and characterization of a new water-soluble cavitand **1**. The container features 2-aminobenzimidazole panels at the “rim” and pyridiniums at the “feet”. In the solid state, a single-crystal X-ray structure of the organic-soluble precursor **2** showed a stable vase form. The structure is stabilized by hydrogen-bonded bridges between adjacent panels through solvents and ions. In aqueous solution, binding of hydrophobic and amphiphilic guest molecules to **1** was investigated using ¹H NMR. Alkanes, alcohols, acids, diols, and diacids formed 1:1 host–guest complexes, and the guest conformations were deduced from characteristic chemical shift changes. In the presence of [Pd(ethylenediamine)(H₂O)₂]NO₃, cavitand **1** formed a complex incorporating two metals. The metal-coordinated cavitand also bound hydrophobic linear alkanes and difluorobenzene isomers in aqueous medium. The metallo-cavitand showed shape and size selectivity and was used to separate *o*-difluorobenzene from its isomers as observed by ¹⁹F NMR spectroscopy. The primary amino function of the cavitands offers possibilities for further elaboration to covalent clusters of these container compounds.



Hydrophobic and Metal-coordinated Effects into Selectivity

Cavitands are container host molecules with an open end and movable walls that allow uptake and release of guests. Since their introduction by Cram^{1,2} and Dalcanale,³ cavitands are widely used in studies of molecular recognition and confinement.^{4,5} Many structural variants have been reported⁶ on the basis of the resorcinarene platform and with a wide variety of aromatic panels or “walls”.^{7–9} They exist in two different shapes: the receptive “vase” shape and unreceptive “kite” (or velcrand) shape.¹ Both shapes often exist in dimeric forms known as capsules and velcrands, respectively. The guest molecules fill the space of the cavities and solvate the interior surfaces of the hosts. Additional functional groups that create further possibilities for selectivity in guest recognition can be introduced on the upper rim.⁶

Among many attempts to control the shape and size of the space in cavitands,^{10,11} a recent success involves Pd(II) metal coordination on the upper rim.^{12,13} The coordination of two Pd(II) metal atoms by adjacent quinoxaline panels distorts the shape of the cavitand from a time-averaged C_{4v} symmetry to C_{2v} and rigidifies the walls. The cross section of the cavity changes from square to a rhombus and alters the guest selectivity. In this work, we expand the use of metal complexation by using 2-aminobenzimidazoles for the walls of the cavitands (Figure 1). We find that metal binding stabilizes the vase forms (Figure 1), creates selective recognition for difluorobenzene isomers, and offers possibilities for further expansion of cavitand structures through the primary amino group.^{14,15}

The new cavitand **1** was synthesized from the well-known precursor, octamino cavitand **3**¹⁶ (Figure S1), by reaction with BrCN in the presence of K₂CO₃ (see the detailed procedure in the Supporting Information). Aminobenzimidazole cavitand **2** was isolated in excellent yield and was converted into water-soluble cavitand **1** by placing pyridinium “shoes” on the feet. All of the cavitand products were characterized by ¹H and ¹³C NMR spectroscopy and high-resolution mass spectrometry (HRMS) (Figures S1–S10).

Single crystals of cavitand **2** suitable for X-ray diffraction analysis were obtained from the diffusion of ether into its DMSO solution. The crystal structure obtained is given in panels a and b of Figure 2 (see detailed data in Table S1 and Figure S106). The cavitand crystallized in a vase conformation with four counter bromide anions and three DMSO solvent molecules (Figure 2). The bromide ions and the dimethyl sulfoxide solvent molecules alternate along the rim of the (protonated) exocyclic nitrogen atoms (Figure 2b,c). The exocyclic NH₂’s also interact with Br[–] or O(solvent). Cartoon representations of hydrogen bonding interactions along the

Received: April 6, 2021

Published: June 11, 2021



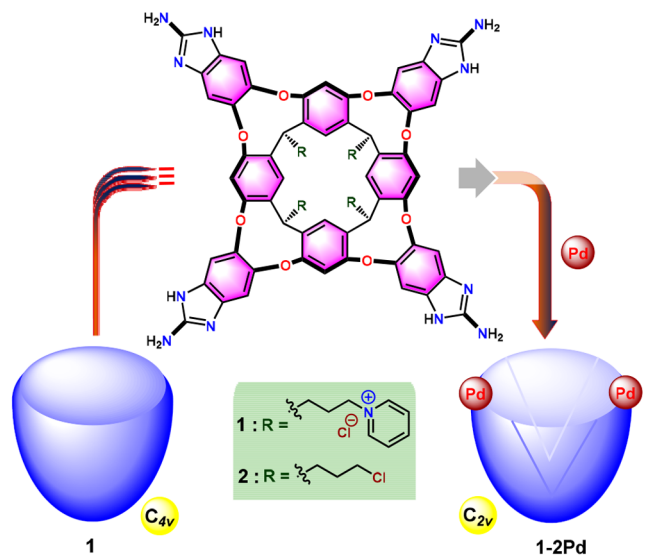


Figure 1. Structure and cartoons of the cavitands containing 2-aminobenzimidazoles at the upper rim (**1**) and the palladium complex **1–2Pd**.

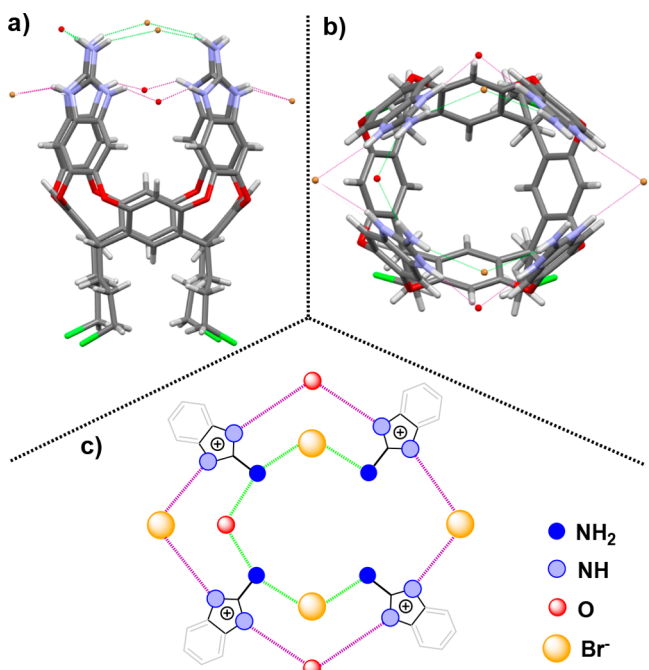


Figure 2. Single-crystal structure of cavitand 2: (a) side view, (b) top view, and (c) cartoon representation of the packing arrangement and hydrogen bonding interactions between cavitand and solvent (DMSO) or ions (Br⁻). Noncoordinated solvents, counterions, and co-crystallized molecules have been omitted for the sake of clarity. Thermal ellipsoids are drawn at a 50% probability level.

outer rim are shown in Figure 2c. The heavy atom H-bonding distances are ~ 2.4 – 2.7 Å for N–H···Br⁻ and ~ 2.04 – 2.6 Å for N–H···O(solvent); these noncovalent interactions are reasonable for hydrogen bonds that stabilize the vase conformation.

In solution, cavitand **1** was found in the vase form in DMSO-*d*₆ and in the vase and velcrand conformations in D₂O (Figures S4–S8). The vase form is recognized by its methine proton's characteristic chemical shift at 5.5 ppm, whereas in

the kite or velcrand form, this signal appears below 4.7 ppm. Cavitand **1** showed good solubility in water (D₂O) at concentrations of ≤ 20 mM.

Cavitand **1** presents the hydrophobic environment of the cavity depths and the polar surfaces of the 2-amino-benzimidazole upper rim simultaneously to its bound guest molecules. The *pK_a* of such benzo-fused guanidines is near neutrality,^{17–19} so the protonation states and the number of charges on the rim are fluid in solution and difficult to determine. Buffers typically “salt out” such cavitands, so D₂O solutions were used directly. We examined the versatility of binding of cavitand **1** to typical guests like *n*-alkanes, cyclic alkanes and ketones, mono/dialcohols, and carboxylic acids using NMR spectroscopy (Figures S11–S72), and the binding modes are proposed through cartoon representations. The in/out exchange of guests is relatively slow on the NMR time scale, and the guests' signals are shifted upfield (up to ~ 5 ppm) by the shielding provided by the eight surrounding aromatic panels of **1**.

For *n*-alkanes, binding behaviors and patterns varied depending on length. Short alkanes show broadened and clustered signals, while longer guests show sharpened peaks at wider ranges of chemical shifts (Figure 3a and Figures S12–S22). This trend reflects the average position of a guest nucleus, but there is considerable motion of the guest in the space: short alkanes can move freely, medium sizes can tumble rapidly “end over end”, while longer alkanes fold and undergo “yo-yo” motions.^{20–23} Guest conformations are also subject to length: the shortest alkanes (C5–C8) move through tumbling rapidly, the medium alkanes (C9–C12) better fill the space and solvate the aromatic panels by coiling, tumbling slowly, and the longer alkanes (C13–C15) fold in J shapes to reduce surface areas exposed to the aqueous environment and undergo “yo-yo” motions (Figure 3a,b). The shape of the space in the cavity—from a rigid, tapered floor near the resorcinarene to the broadened, flexible opening at the rim—also influences the guest orientation. Typically, a methyl group fits into the tapered space at the bottom where the maximum magnetic anisotropy is experienced ($\Delta\delta \geq -4$ ppm), while polar groups are closer to the rim where little or no perturbation of their NMR signals is experienced. The predictable increase in the magnetic effect with depth in similar cavitands has been described in detail elsewhere.²⁴

Cycloalkanes and cyclic ketones also form 1:1 host–guest complexes in aqueous medium and illustrate the expected NMR chemical shift ($\Delta\delta$) trends described above (Figure 3c,d and Figures S25–S36). Cycloalkanes such as cycloheptane and cyclooctane show sharp and single resonances indicating a dynamic process that makes all of their CH₂ groups experience the same magnetic environment. This is accomplished by motion along all three axes: rapid rolling, tumbling, and flipping of the guest on the NMR time scale that simplify the signals of the cavitand. The motions ensure an average C_{4v} symmetry for the entire complex. The difference in chemical shifts (0.3 ppm) indicates that the average position of a cyclooctane CH₂ is higher in the cavitand. For the respective cyclic ketones, the spread of the nondescript (β and γ) CH₂ signals shows a preferred orientation of the guest in the cavity as shown in panels c and d of Figure 3. The carbonyl group spends most of its time near the polar environment of the rim.

Amphiphilic molecules such as long chain alcohols and carboxylic acids (Figure 4a,b and Figures S37–S50) showed good binding to **1**, but shorter alcohols and carboxylic acids

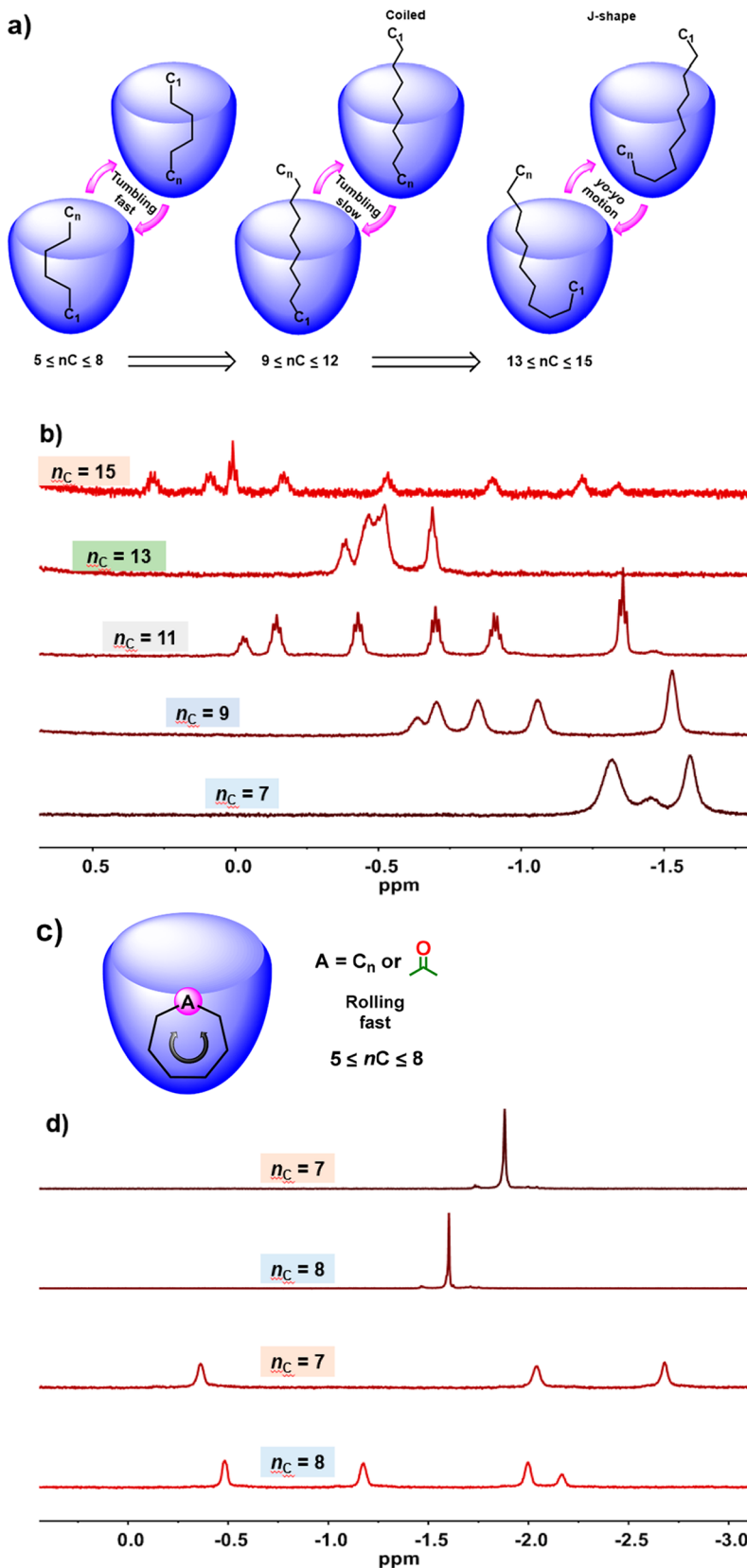


Figure 3. (a) Cartoon representation for the binding modes and/or patterns of various n -alkanes ($n_C = 7, 9, 11, 13$, and 15) to **1** and (b) partial ^1H NMR spectra of the respective complexes. (c) Cartoon representation for the binding patterns of various cyclic alkanes ($n_C = 7$ and 8) and cyclic ketones ($n_C = 7$ and 8). (d) Partial ^1H NMR spectra (600 MHz, D_2O , 298 K) of the respective complexes. [**1**] = 1 mM in D_2O ; [**G**] = 100 mM in acetone.

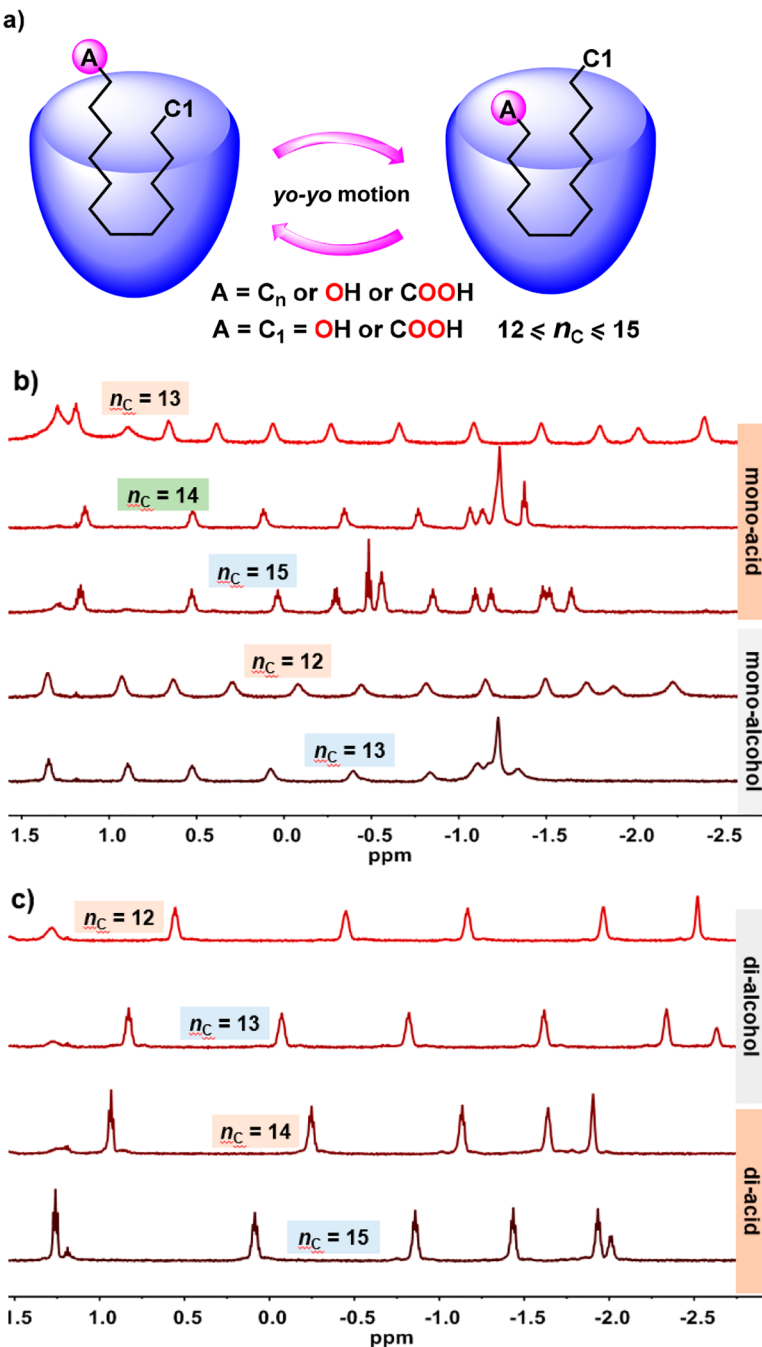


Figure 4. (a) Cartoon representation for the binding modes and patterns of various monoalcohols ($n_{\text{C}} = 12$ and 13), monoacid ($n_{\text{C}} = 13, 14$, and 15), dialcohol ($n_{\text{C}} = 12$ and 13), and diacid ($n_{\text{C}} = 14$ and 15) to **1**. (b and c) Respective partial ^1H NMR spectra (600 MHz, D_2O , 298 K) of the complexes. $[\mathbf{1}] = 1 \text{ mM}$ in D_2O ; $[\mathbf{G}] = 100 \text{ mM}$ in acetone.

with eight or nine carbon atoms with good water solubility were poor guests. As the guest chain length increases, the triplet signal for the terminal CH_3 moves downfield: from -2.3 ppm for acid (C13) to -1.5 ppm (C14) to -0.5 ppm (C15). This trend indicates folding that brings the CH_3 closer to the rim because the polar end is expected to remain fixed at the aqueous interface. The same trend is observed for the primary alcohols (Figure 4a,b and Figures S45–S50).

Other amphiphilic guests like α,ω -diols and dicarboxylic acids showed good binding to **1**, even though they enjoy better water solubility (Figure 4a,c and Figures S51–S62). The highest upfield signals of the diols at around -2.6 to -2.72

ppm ($\Delta\delta \sim 4.0 \text{ ppm}$) indicate a CH_2 is mostly fixed at the bottom of the cavity, and the guests maintain (time-averaged) symmetrically folded U-shaped conformations. The acids also fold to fill the cavity's space, but the deepest signal at approximately -2 ppm indicates that the associated CH_2 is not fixed. Rapid "yo-yo" motions between J-shaped conformations are consistent with their spectra (Figure 4a,c and Figures S63–S71).

Container molecules stabilized by metal coordination play an important role in supramolecular chemistry,^{25–28} and their effects on confined molecules continue to be explored.^{29,30} We recently introduced metal coordination to cavitands through

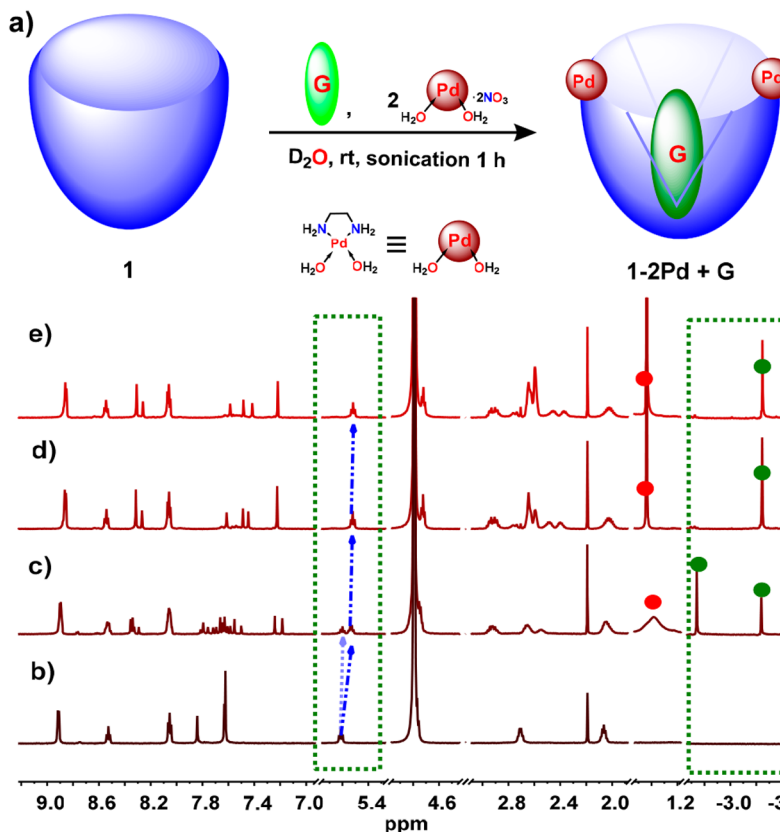


Figure 5. (a) Cartoon representation for metallo-cavitand **1–2Pd** formation in aqueous medium. Partial ^1H NMR spectra (600 MHz, D_2O , 298 K) of metallo-cavitand **1–2Pd** formation. (b) Cavitand **1** (1 mM) and cyclopentane (excess) and addition of a Pd(II) precursor: (c) 1, (d) 2, and (e) 3 equiv (free cyclopentane signal denoted as red circles and bound cyclopentane signals denoted as green circles).

chelation with the nitrogen atoms of adjacent quinoxaline walls.¹² Coordination to Pd(II) alters the shape and size of the cavity, as determined by its modified binding selectivity. The Pd(II) metal coordination of **1** was monitored by using ^1H NMR titration with 1–3 equiv of a Pd(II) precursor [$\text{Pd}(\text{EDA})(\text{H}_2\text{O})_2 \cdot 2\text{NO}_3$] (EDA = ethylenediamine) with the results shown in Figure 5. Without Pd(II), no binding of cyclopentane occurs, but maximum complexation of this guest is seen when the two metal atoms are present. The nitrogen atoms of the benzimidazole rim are appropriate coordination sites and lead to **1–2Pd**, with a 1:2 cavitand:metal ratio. Appropriate changes are seen in the aromatic region of NMR spectra of the container.^{31,32} Apparently, Pd(II) coordination stabilizes the host–guest complex by rigidifying the cavitand. The cyclopentane complex signals at -2.7 to -3.3 ppm [$\Delta\delta = 4.1$ – 4.7 ppm (Figure 5c)] and the corresponding methine proton’s characteristic chemical shift at ~ 5.5 ppm are clear evidence that two complexes exist in solution. The simplest interpretation consistent with the spectra is that a transient complex with one Pd and one cyclopentane exists when the concentration of the Pd precursor is low (Figure 5).¹²

We examined a number of guests binding in D_2O using *in situ*-generated cavitand **1–2Pd**, and relative binding cartoon models are depicted in Figure 6a. The binding results of linear alkanes and monoalkyl alcohols are given in Figure 6 and Figures S73–S91. Unlike cavitand **1**, normal alkanes (C6–C13) are bound in **1–2Pd** in a linear extended conformation (Figure 6b and Figures S12–S19). The shortest guest (CS) showed a unique conformation behavior in the confined space of **1–2Pd** with broad signals indicating the complex is

dynamic. One methyl group of the *n*-alkanes shows the maximum upfield shift ($\Delta\delta = -5.2$ ppm) as it fits into the tapered bottom of the cavity. Increasing the chain length even to C13 showed a similar binding pattern. Apparently, the Pd coordination makes the cavitand **1–2Pd**’s cavity narrower; the guest nuclei are closer to the walls and experience larger upfield shifts in an extended conformation.¹²

Longer chain ($n_{\text{C}} > 5$) alkanes with polar termini (-OH, amphiphilic guests) were bound to **1–2Pd** with an identical extended arrangement and completely restricted tumbling or other motions (Figure 6a). The methyl groups and the next four carbons experienced the same magnetic environments as alkanes (Figure 6c and Figures S83–S91). As the number of alkyl carbon atoms increases, the solubility of the guest decreases and signals become weak as they fail to compete with the cosolvent acetone. The identical signal patterns of the guests in **1–2Pd** (Figure 6) provide a consistent map of chemical shifts for alkyl groups packed into the pinched cavity.

Finally, we applied the metallo-cavitand’s selective binding to the separation of halobenzene isomers.³³ As these regioisomers have close boiling points, various difficulties are encountered in their separation.³³ Generally, azeotropic distillation and extractive distillation are used as classical methods; these are energy-intensive. Separations based on molecular recognition are scarce, but recently, a promising method involves pillarenes: in the crystalline state, open-ended pillarenes offer a faster absorption of *ortho* isomers based on shape complementarity.^{34–38} Metallo-cavitand **1–2Pd** was examined for binding selectivity (Figure 7) and separation of regioisomers of difluorobenzene in an aqueous medium using

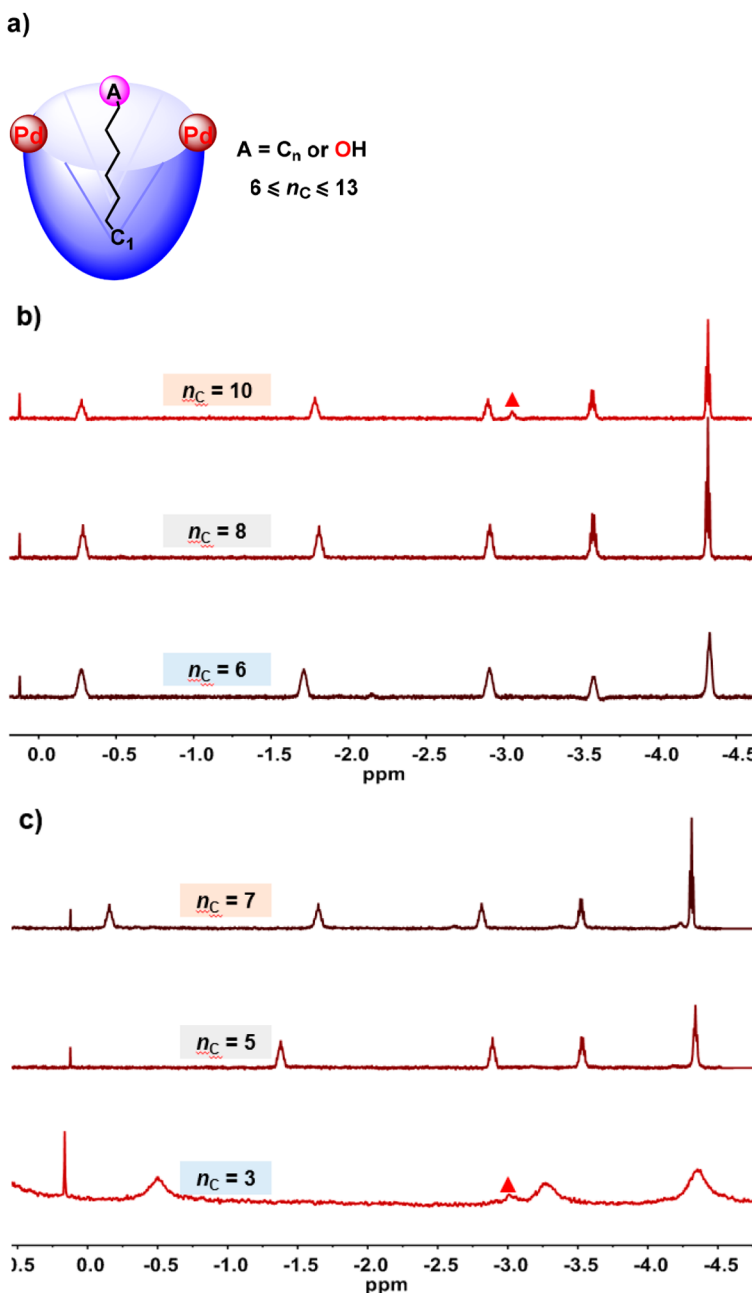


Figure 6. (a) Cartoon representation for the binding modes of various *n*-alkanes and primary alcohols to **1–2Pd**. Partial ¹H NMR spectra (600 MHz, D₂O, 298 K) of the complexes formed between host **1–2Pd** (1 mM) and (b) excess *n*-alkanes (*n*_C = 6, 8, and 10) and (c) excess primary alcohols (*n*_C = 3, 5, and 7). The residual bound acetone solvent signals are marked with red triangles.

an extraction cycle (Figure S100). This separation was used to selectively obtain the *o*DFB with >99.9% purity without large investments in energy or costly instrumentation.

First, binding of the difluorobenzene regioisomers to **1–2Pd** was studied by ¹⁹F NMR spectroscopy at 298 K. Sonication of **1–2Pd** in D₂O with any of the DFB isomers gave stoichiometric complexes, and competitive binding experiments showed the stability decreased in the following order: *o*-difluorobenzene > *p*-difluorobenzene ≫ *m*-difluorobenzene (Figure 7 and Figures S97–S99). The proposed 1:1 **1–2Pd**:*o*/*m/p*DFB binding cartoon models are given in Figure 7a, suggesting that selective recognition is a result of size and shape complementarity.

When a mixture of difluorobenzene isomers was suspended in a solution of **1–2Pd** in D₂O, *o*DFB was captured (Figure S100) and transferred into the aqueous solution (Figure S100, step A), leaving the other two isomers in the organic phase [CHCl₃? (Figure S100, step B)]. The captured *o*DFB was extracted from the aqueous solution with chloroform (Figure S100, step C, and Figures S101 and S102). The quantity of *o*DFB was determined using DMSO as an internal standard, which showed an equivalent recovery of *o*DFB (Figure S100, step D, and Figures S102 and S103). The host exhibited a stable vase conformation with CDCl₃ inside after extraction (Figure S104). The aqueous solution of **1–2Pd** was reused to perform another cycle.

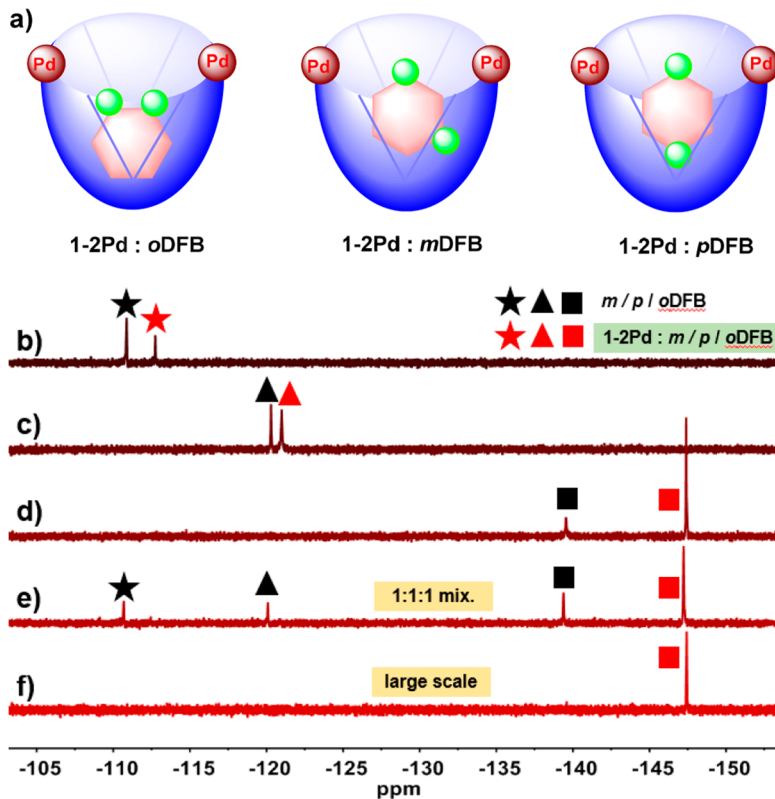


Figure 7. (a) Proposed models of binding of the difluorobenzene regioisomers to metallo-cavitand **1–2Pd**. The difluorobenzenes rotate quickly in the cavity, and the ^{19}F NMR spectra show only the time-averaged positions of F atoms in the cavity; the cartoons are merely suggestions. Comparative partial ^{19}F NMR (564 MHz, D_2O , 298 K) spectra of the complexes formed between host **1–2Pd** (1 mM) and DFB regioisomers: (b) bound *mDFB*, (c) bound *pDFB*, (d) bound *oDFB*, (e) excess 1:1:1 DFB mixture (100 mM in DMSO), and (f) **1–2Pd**. After competition, only *oDFB* was captured by **1–2Pd** in a large scale-up result. The unbound guests are denoted with black markers, and bound guests are denoted with red markers.

CONCLUSIONS

In summary, a new cavitand bearing 2-aminobenzimidazole walls and pyridinium feet was prepared and characterized. The cavitand showed good solubility in water and binding affinity for small hydrophobic and hydrophilic organic guests molecules, including *n*-alkanes, cycloalkanes, cyclic ketones, *n*-alcohols, carboxylic acids, diols, and diacids. The presence of benzimidazole walls allowed for the coordination of two Pd(II) ions; the metal derivative enhanced guest binding, and water-soluble guests could be complexed. The reorganized shape of the space in **1–2Pd** showed selectivity for *o*-difluorobenzene over its isomers, and a simple separation scheme based on extraction was developed. The convenience of the cavitand's synthesis, high water solubility, and possibilities for elaboration make it a promising platform for molecular recognition in aqueous environments.

EXPERIMENTAL SECTION

General Experimental Methods. All analytical grade solvents and reagents purchased from commercial sources were used without further purification. BrCN was purchased from Tansoole Company Shanghai Ltd. ^1H , $^{13}\text{C}\{^1\text{H}\}$, and ^{19}F NMR analyses were performed using a Bruker AVANCE III HD 600 MHz spectrophotometer at 298 K, and commercially available deuterated solvents were used in the analysis. Positive ion high-resolution mass analyses were performed on a Bruker solari X machine. A single crystal was measured with a Bruker D8 VENTURE PHOTON II diffractometer. GC analyses were performed using a Shimadzu GC-2030AF chromatograph. The synthesis of **3** was reported previously.¹⁶

Synthesis of Tetra(chloropropyl) 2-Aminobenzimidazole Cavitand 2. Tetra(chloropropyl) octaamino cavitand HCl salt **3** (751 mg, 0.5 mmol) and methanol (100 mL) were placed in a 250 mL round-bottom flask, treated with 8 equiv of K_2CO_3 (1106 mg, 4.0 mmol), and then filtered to obtain free *o*-phenylenediamine as a solid. The solid was dispersed in methanol (20 mL) (through sonication), and then 4.4 equiv of solid BrCN (467 mg, 2.2 mmol) was added. The reaction mixture was allowed to warm slowly to 60 °C in an oil bath and stirred overnight (12 h), during which a white solid has precipitated. The solid was filtered and washed thoroughly with methanol (20 mL). Product **2** was obtained as a pale yellow solid (621 mg, 95% yield) and pure enough for use in the next step. ^1H NMR (600 MHz, $\text{DMSO}-d_6$): δ 12.01 (s, 8H), 8.55 (s, 8H), 7.92 (s, 4H), 7.78 (s, 8H), 7.71 (s, 4H), 5.55 (t, J = 8.0 Hz, 4H), 3.73 (t, J = 6.6 Hz, 8H), 2.47 (m, 8H), 1.71 (m, J = 6.7 Hz, 8H). $^{13}\text{C}\{^1\text{H}\}$ NMR (150 MHz, $\text{DMSO}-d_6$): δ 155.6, 150.8, 148.5, 135.0, 126.7, 125.1, 117.1, 106.9, 54.7, 44.9, 32.7, 30.9, 29.0. HRMS (ESI) m/z : [M + H]⁺ calcd for $\text{C}_{68}\text{H}_{57}\text{Cl}_4\text{N}_{12}\text{O}_8$ 1309.3176, found 1309.3159.

Synthesis of Water-Soluble 2-Aminobenzimidazole Cavitand 1. First, 100 mg of **2** was taken up in 10 mL of pyridine and heated at 120 °C in an oil bath for 12 h under a nitrogen atmosphere. The mixture was cooled to room temperature; 50 mL of acetone was added, and the mixture was stirred for 1 h. A pale solid precipitated and was filtered and washed with acetone (50 mL). The recovered solid was suspended in 30 mL of acetone, vigorously stirred, and heated at 60 °C in an oil bath for 4 h. The obtained suspension was cooled to room temperature, filtered, washed thoroughly with acetone (20 mL), and dried under high vacuum. The yield of the pale solid was 120 mg (97%). ^1H NMR (600 MHz, $\text{DMSO}-d_6$): δ 12.17 (s, 6H), 9.40 (d, J = 6.1 Hz, 8H), 8.76 (s, 5H), 8.65 (t, J = 7.8 Hz, 5H), 8.27 (t, J = 6.9 Hz, 8H), 7.94 (s, 6H), 7.79 (s, 4H), 7.77 (s, 8H), 5.41 (t, J = 8.4 Hz, 4H), 4.82 (t, J = 6.7 Hz, 8H), 2.68 (m, 8H), 1.89 (m, J

= 8.1, 8H). $^{13}\text{C}\{\text{H}\}$ NMR (150 MHz, DMSO- d_6): δ 155.67, 149.5, 148.26, 145.7, 144.9, 134.9, 128.2, 125.5, 123.9, 117.1, 106.9, 61.3, 33.4, 28.7, 28.6. HRMS (ESI) m/z : [M + 3H] $^{3+}$ calcd for $\text{C}_{88}\text{H}_{79}\text{N}_{16}\text{O}_8\text{Cl}_4$ 1627.5021, found 1627.4955. [M + 3Na] $^{3+}$ calcd for $\text{C}_{88}\text{H}_{76}\text{N}_{16}\text{O}_8\text{Cl}_4\text{Na}_3$ 1693.4479, found 1693.4893.

General Procedure for NMR Binding Analyses. Compound 1 (1 mM in D_2O , 0.5 mL) was placed in a NMR tube, and excess pure guests such as *n*-alkane, cyclic guests, *n*-alcohol/acid, and diacid/alcohol (0.2 μL) were added to the tube and then shaken well to mix the guest in water. The sample was then sonicated for 1 h and analyzed by ^1H NMR spectroscopy at 298 K.

General Procedure for NMR Titration Experiments. One (1 mM in D_2O , 0.5 mL) was taken in a NMR tube, and excess pure cyclopentane (0.2 μL) was added, which is added with gradually increasing equivalents of the Pd(II) precursor complex.¹² The tube was shaken well to mix the guest in water, then sonicated for 1 h, and analyzed by ^1H NMR spectroscopy at 298 K.

General Procedure for the Binding Properties in D_2O Using the *In Situ* Generation of Cavitand 1–2Pd. Compound 1 (1 mM in D_2O , 0.5 mL) and 2.0 equiv of a Pd(EDA)(H_2O) $_2\text{NO}_3$ solution in D_2O were placed in a NMR tube, and excess pure guests such as *n*-alkane or *n*-alcohol (0.3 μL or 0.3 mg) were added. The tube was shaken well to mix the guest in water, sonicated for 1 h, and analyzed by ^1H NMR spectroscopy at 298 K.

General Procedure for the Binding of Difluorobenzenes Using *In Situ* Generation Cavitand 1–2Pd. Compound 1 (1 mM in D_2O , 0.5 mL) and 2.0 equiv of a Pd(EDA)(H_2O) $_2\text{NO}_3$ solution in D_2O were placed in a NMR tube, and an excess of difluorobenzene (0.3 μL or 0.3 mg) or (100 mM in DMSO) was added. The tube was shaken well to mix the guest in water. The sample was sonicated for 1 h and analyzed by ^{19}F NMR spectroscopy at 298 K.

ASSOCIATED CONTENT

Supporting Information

The Supporting Information is available free of charge at <https://pubs.acs.org/doi/10.1021/acs.joc.1c00794>.

Related procedures, general experimental, crystallographic data, and original ^1H , $^{13}\text{C}\{\text{H}\}$, and ^{19}F NMR spectra ([PDF](#))

Accession Codes

CCDC 2074472 contains the supplementary crystallographic data for this paper. These data can be obtained free of charge via www.ccdc.cam.ac.uk/data_request/cif, or by emailing data_request@ccdc.cam.ac.uk, or by contacting The Cambridge Crystallographic Data Centre, 12 Union Road, Cambridge CB2 1EZ, UK; fax: +44 1223 336033.

AUTHOR INFORMATION

Corresponding Author

Yang Yu – Center for Supramolecular Chemistry & Catalysis and Department of Chemistry, College of Science, Shanghai University, Shanghai 200444, China; orcid.org/0000-5698-3534; Email: yangyu2017@shu.edu.cn

Authors

Hui-Bin Zhang – Center for Supramolecular Chemistry & Catalysis and Department of Chemistry, College of Science, Shanghai University, Shanghai 200444, China

Kuppusamy Kanagaraj – Center for Supramolecular Chemistry & Catalysis and Department of Chemistry, College of Science, Shanghai University, Shanghai 200444, China

Julius Rebek, Jr. – Center for Supramolecular Chemistry & Catalysis and Department of Chemistry, College of Science, Shanghai University, Shanghai 200444, China; Skaggs Institute for Chemical Biology and Department of Chemistry,

The Scripps Research Institute, La Jolla, California 92037, United States; orcid.org/0000-0002-2768-0945

Complete contact information is available at: <https://pubs.acs.org/10.1021/acs.joc.1c00794>

Notes

The authors declare no competing financial interest.

ACKNOWLEDGMENTS

This work was supported by the National Natural Science Foundation of China (21801164 and 22071144) and Shanghai University (13-G210-19-230). Y.Y. thanks the Program for Professor of Special Appointment (Dongfang Scholarship) of the Shanghai Education Committee.

REFERENCES

- Moran, J. R.; Ericson, J. L.; Dalcanale, E.; Bryant, J. A.; Knobler, C. B.; Cram, D. J. Vases and Kites as Cavitands. *J. Am. Chem. Soc.* **1991**, *113* (15), 5707–5714.
- Moran, J. R.; Karbach, S.; Cram, D. J. Cavitands: Synthetic Molecular Vessels. *J. Am. Chem. Soc.* **1982**, *104* (21), 5826–5828.
- (a) Dalcanale, E.; Soncini, P.; Bacchilega, G.; Uguzzoli, F. Selective Complexation of Neutral Molecules in Organic Solvents. Host-Guest Complexes and Cavitates between Cavitands and Aromatic Compounds. *J. Chem. Soc., Chem. Commun.* **1989**, *8*, 500–502. (b) Petroselli, M.; Chen, Y.; Rebek, J., Jr.; Yu, Y. Binding and Reactivity in Deep Cavitands Based on Resorcin[4]arene. *Green Synth. and Catal.* **2021**, *2*, 123–130.
- Heinz, T.; Rudkevich, D. M.; Rebek, J., Jr. Pairwise Selection of Guests in a Cylindrical Molecular Capsule of Nanometre Dimensions. *Nature* **1998**, *394* (6695), 764–766.
- Rahman, F. U.; Tzeli, D.; Petsalakis, I. D.; Theodorakopoulos, G.; Ballester, P.; Rebek, J., Jr.; Yu, Y. Chalcogen Bonding and Hydrophobic Effects Force Molecules into Small Spaces. *J. Am. Chem. Soc.* **2020**, *142* (12), 5876–5883.
- Wishard, A.; Gibb, B. C. A Chronology of Cavitands. *Calixarenes and Beyond.* **2016**, 195–234.
- Rahman, F. U.; Feng, H. N.; Yu, Y. A New Water-Soluble Cavitand With Deeper Guest Binding Properties. *Org. Chem. Front.* **2019**, *6* (7), 998–1001.
- Bryant, J. A.; Knobler, C. B.; Cram, D. J. Organic Molecules Dimerize with High Structural Recognition When Each Possesses a Large Lipophilic Surface Containing Two Preorganized and Complementary Host and Guest Regions. *J. Am. Chem. Soc.* **1990**, *112* (3), 1254–1255.
- Cram, D. J.; Choi, H. J.; Bryant, J. A.; Knobler, C. B. Solvophobic and Entropic Driving Forces for Forming Velcraplexes, Which Are Four-Fold, Lock-Key Dimers in Organic Media. *J. Am. Chem. Soc.* **1992**, *114* (20), 7748–7765.
- Frei, M.; Diederich, F.; Tremont, R.; Rodriguez, T.; Echegoyen, L. Tetrathiafulvalene (TTF)-Bridged Resorcin[4]arene Cavitands: Towards New Electrochemical Molecular Switches. *Helv. Chim. Acta* **2006**, *89* (9), 2040–2057.
- Purse, B. W.; Rebek, J., Jr. Functional cavitands: Chemical reactivity in structured environments. *Proc. Natl. Acad. Sci. U. S. A.* **2005**, *102* (31), 10777–10782.
- Rahman, F. U.; Li, Y. S.; Petsalakis, I. D.; Theodorakopoulos, G.; Rebek, J., Jr.; Yu, Y. Recognition with Metallo Cavitands. *Proc. Natl. Acad. Sci. U. S. A.* **2019**, *116* (36), 17648–17653.
- Rahman, F. U.; Yang, J. M.; Wan, Y. H.; Zhang, H. B.; Petsalakis, I. D.; Theodorakopoulos, G.; Rebek, J., Jr.; Yu, Y. Binding Selectivity and Separation of p-Functionalized Toluenes with a Metallo-Cavitand in Water. *Chem. Commun. (Cambridge, U. K.)* **2020**, *56* (51), 6945–6948.
- He, X.; Lakkaraju, S. K.; Hanscom, M.; Zhao, Z.; Wu, J.; Stoica, B.; MacKerell, A. D., Jr.; Faden, A. I.; Xue, F. Acyl-2-amino-

- benzimidazoles: a Novel Class of Neuroprotective Agents Targeting mGluRs. *Bioorg. Med. Chem.* **2015**, *23* (9), 2211–2220.
- (15) Liu, S.; Russell, D. H.; Zinnel, N. F.; Gibb, B. C. Guest Packing Motifs within a Supramolecular Nanocapsule and a Covalent Analogue. *J. Am. Chem. Soc.* **2013**, *135* (11), 4314–4324.
- (16) Mosca, S.; Yu, Y.; Rebek, J., Jr. Preparative Scale and Convenient Synthesis of a Water-Soluble Deep Cavitand. *Nat. Protoc.* **2016**, *11* (8), 1371–1387.
- (17) Dash, A. C.; Panda, D.; Dash, B. Kinetics & Equilibrium Studies on Reversible Formation of N-Salicylidene 2-Aminomethylbenzimidazole & Its Copper(II) Complex. *Indian J. Chem.* **1986**, *25A* (2), 141–146.
- (18) Dash, A. C.; Acharya, A. N.; Sahoo, R. K. Binary and Ternary Complexes of Nickel(II) with 2-Aminomethylbenzimidazole and Salicylaldehyde: Kinetic and Equilibrium Studies. *J. Chem. Soc., Dalton Trans.* **1994**, *24*, 3727–3731.
- (19) Sierra-Zenteno, A.; Galán-Vidal, C. A.; Tapia-Benavides, R. Acid-base Equilibrium Studies of 2-(Aminomethyl)benzimidazole in Aqueous Solution. *Rev. Soc. Quím. Mex.* **2002**, *46* (2), 125–130.
- (20) Gan, H.; Benjamin, C. J.; Gibb, B. C. Nonmonotonic Assembly of a Deep-Cavity Cavitand. *J. Am. Chem. Soc.* **2011**, *133* (13), 4770–4773.
- (21) Zhang, K. D.; Ajami, D.; Rebek, J., Jr. Hydrogen-Bonded Capsules in Water. *J. Am. Chem. Soc.* **2013**, *135* (48), 18064–18066.
- (22) Zhang, K. D.; Ajami, D.; Gavette, J. V.; Rebek, J., Jr. Complexation of Alkyl Groups and Ghrelin in a Deep, Water-Soluble Cavitand. *Chem. Commun. (Cambridge, U. K.)* **2014**, *50* (38), 4895–4897.
- (23) Hooley, R. J.; Biros, S. M.; Rebek, J., Jr. Normal Hydrocarbons Tumble Rapidly in a Deep, Water-soluble Cavitand. *Chem. Commun. (Cambridge, U. K.)* **2006**, *5*, 509–510.
- (24) Yu, Y.; Rebek, J., Jr. Reactions of Folded Molecules in Water. *Acc. Chem. Res.* **2018**, *51* (12), 3031–3040.
- (25) Fujita, M.; Tominaga, M.; Hori, A.; Therrien, B. Coordination Assemblies from a Pd(II)-Cornered Square Complex. *Acc. Chem. Res.* **2005**, *38* (4), 369–378.
- (26) Pluth, M. D.; Raymond, K. N. Reversible Guest Exchange Mechanisms in Supramolecular Host-guest Assemblies. *Chem. Soc. Rev.* **2007**, *36* (2), 161–171.
- (27) Cai, L. X.; Li, S. C.; Yan, D. N.; Zhou, L. P.; Guo, F.; Sun, Q. F. Water-Soluble Redox-Active Cage Hosting Polyoxometalates for Selective Desulfurization Catalysis. *J. Am. Chem. Soc.* **2018**, *140* (14), 4869–4876.
- (28) Wang, L. J.; Li, X.; Bai, S.; Wang, Y. Y.; Han, Y. F. Self-Assembly, Structural Transformation, and Guest-Binding Properties of Supramolecular Assemblies with Triangular Metal-Metal Bonded Units. *J. Am. Chem. Soc.* **2020**, *142* (5), 2524–2531.
- (29) Zhu, Y. J.; Gao, Y.; Tang, M. M.; Rebek, J., Jr.; Yu, Y. Dimeric Capsules Self-Assembled Through Halogen and Chalcogen Bonding. *Chem. Commun. (Cambridge, U. K.)* **2021**, *57* (13), 1543–1549.
- (30) Grommet, A. B.; Feller, M.; Klajn, R. Chemical Reactivity under Nanoconfinement. *Nat. Nanotechnol.* **2020**, *15* (4), 256–271.
- (31) Galan, A.; Ballester, P. Stabilization of Reactive Species by Supramolecular Encapsulation. *Chem. Soc. Rev.* **2016**, *45* (6), 1720–1737.
- (32) Wang, K.; Cai, X.; Yao, W.; Tang, D.; Kataria, R.; Ashbaugh, H. S.; Byers, L. D.; Gibb, B. C. Electrostatic Control of Macrocyclization Reactions within Nanospaces. *J. Am. Chem. Soc.* **2019**, *141* (16), 6740–6747.
- (33) Zhang, H. N.; Lu, Y.; Gao, W. X.; Lin, Y. J.; Jin, G. X. Selective Encapsulation and Separation of Dihalobenzene Isomers with Discrete Heterometallic Macrocages. *Chem. - Eur. J.* **2018**, *24* (71), 18913–18921.
- (34) Li, E. R.; Zhou, Y. J.; Zhao, R.; Jie, K. C.; Huang, F. H. Dihalobenzene Shape Sorting by Nonporous Adaptive Crystals of Perbromoethylated Pillararenes. *Angew. Chem., Int. Ed.* **2019**, *58* (12), 3981–3985.
- (35) Xia, D. Y.; Wang, P.; Ji, X. F.; Khashab, N. M.; Sessler, J. L.; Huang, F. H. Functional Supramolecular Polymeric Networks: The Marriage of Covalent Polymers and Macrocycle-Based Host-Guest Interactions. *Chem. Rev.* **2020**, *120* (13), 6070–6123.
- (36) Zhang, G.; Emwas, A.-H.; Shahul Hameed, U. F.; Arold, S. T.; Yang, P.; Chen, A.; Xiang, J.-F.; Khashab, N. M. Shape-Induced Selective Separation of Ortho-substituted Benzene Isomers Enabled by Cucurbit[7]uril Host Macrocycles. *Chem.* **2020**, *6* (5), 1082–1096.
- (37) Zhang, G.; Moosa, B.; Chen, A.; Khashab, N. M. Separation and Detection of meta- and ortho-Substituted Benzene Isomers by Using a Water-Soluble Pillar[5]arene. *ChemPlusChem* **2020**, *85* (6), 1244–1248.
- (38) Wu, G. C.; Wang, C. Y.; Jiao, T. Y.; Zhu, H. T. Z.; Huang, F. H.; Li, H. Controllable Self-Assembly of Macrocycles in Water for Isolating Aromatic Hydrocarbon Isomers. *J. Am. Chem. Soc.* **2018**, *140* (18), 5955–5961.